Journal of Energy Storage 39 (2021) 102587

Contents lists available at ScienceDirect

Journal of Energy Storage

journal homepage: www.elsevier.com/locate/est

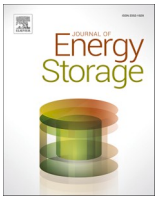

An equivalent circuit model for Vanadium Redox Batteries via hybrid extended Kalman filter and Particle filter methods

Bahman Khaki *, Pritam Das

Department of Electrical and Computer Engineering, State University of New York at Binghamton, NY, USA

ARTICLE INFO

Keywords:
Battery capacity estimation
Electrochemical battery model
Energy storage systems
Equivalent circuit model
Extended Kalman filter
Particle filter
State of charge
Vanadium redox flow battery

ABSTRACT

This paper proposes a model for parameter estimation of Vanadium Redox Flow Battery based on both the electrochemical model and the Equivalent Circuit Model. The equivalent circuit elements are found by a newly proposed optimization to minimized the error between the Thevenin and KVL-based impedance of the equivalent circuit. In contrast to most previously proposed circuit models, which are only introduced for constant current charging, the proposed method is applicable for all charging procedures, i.e., constant current, constant voltage, and constant current-constant voltage charging procedures. The proposed model is verified on a nine-cell VRFB stack by a sample constant current-constant voltage charging. As observed, in constant current charging mode, the terminal voltage model matches the measured data closely with low deviation; however, the terminal voltage model shows discrepancies with the measured data of VRFB in constant voltage charging. To improve the proposed circuit model's discrepancies in constant voltage mode, two Kalman filters, i.e., hybrid extended Kalman filter and particle filter estimation algorithms, are used in this study. The results show the accuracy of the proposed equivalent with an average deviation of 0.88% for terminal voltage model estimation by the extended KF-based method and the average deviation of 0.79% for the particle filter-based estimation method, while the initial equivalent circuit has an error of 7.21%. Further, the proposed procedure extended to estimate the state of charge of the battery. The results show an average deviation of 4.2% in estimating the battery state of charge using the PF method and 4.4% using the hybrid extended KF method, while the electrochemical SoC estimation method is taken as the reference. These two Kalman Filter based methods are more accurate compared to the average deviation of state of charge using the Coulomb counting method, which is 7.4%.

1. Introduction

Redox flow batteries (RFBs) are becoming an emerging type of batteries among battery energy storage systems (BESSs), which are used in both standalone or in hybrid systems with Renewable Energy Sources (RES). There are several possible applications for the RFBs in both off-grid (residential or commercial) and grid-tied applications. Among RFBs, Vanadium Redox Flow Batteries (VRFBs) are the most commercialized type of RFBs for large-scale battery applications and in a hybrid system with other types of RESs. This is because of the benefits of the VRFB system, like long cycle life, environmentally friendly chemistry, non-cross-contamination, and the scalability of VRFB, which means adjustable capacity only by varying the volume of electrolyte.

Some previous research studies make VRFBs more feasible and viable to be used in different BESS applications. These research studies on VRFB can be categorized into the battery stack design [1–3], modifications to the electrode [4–6], and electrolyte type [7–9]. Increasing the performance of VRFB systems relies on accurate modeling of VRFBs. The State of Charge (SoC) of the VRFB is more accurate when formulated in relation to Vanadium ion concentrations using the electrochemical model. This is because, in VRFB systems, the electric charge stores in the reservoir tank's electrolyte. In this paper, a new first-order Equivalent Circuit Model (ECM) is proposed for VRFBs which is combined with the electrochemical model of VRFBs. Moreover, the Nernst equation-based terminal voltage estimation is not accurate for VRFBs since it is originally introduced for fuel cells, not for VRFBs [10,11]. The equation needs some modifications to be accurate of VRFBs. According to our study results, the Nernst equation-based terminal voltage model shows discrepancies with our nine-cell VRFB stack experimental data. An accurate model for the terminal voltage of the VRFB stack can lead to a more accurate formulation for energy and power equations of VRFBs. Energy and power equations are essential for optimal charging and flow

* Corresponding author.
E-mail address: bkhaki1@binghamton.edu (B. Khaki).

https://doi.org/10.1016/j.est.2021.102587
Received 8 February 2021; Received in revised form 20 March 2021; Accepted 12 April 2021
Available online 12 May 2021

management of VRFBs during charging and discharging, which leads to a more efficient operation of VRFBs.

The electrochemical models of the VRFB [12–14] are based on the law of conservation of mass and Vanadium ion concentrations. Decoupled electrical and chemical models [15,16] of the VRFB system impose limitations on the resulting models to accurately depict its behavior under closed-loop operations. Therefore both of electrical and chemical models should be considered to model the battery behavior more accurately.

Some research studies so far consider the ECM models for batteries, including the VRFBs [15–19]. However, some of these models did not include all battery parameters like battery terminal voltage, SoC, and battery discharge capacity. Also, most previous ECMs for VRFBs were proposed for Constant Current (CC) charging mode and are not applicable for the Constant Current-Constant Voltage (CCCV) or Constant Voltage (CV) charging procedures. The CCCV charging method is currently using in many off-grid and grid-tied applications. Therefore, it is crucial to study the ECM behavior for the CCCV charging too, which is one of the concerns of this study. The CC charging procedure is not a safe charging procedure compared to the CCCV charging.

A Resistance-Capacitance (RC) equivalent model of VRFB is proposed in [15,16], where the open circuit cell potential and SoC for charge/discharge experiments were measured by extended Kalman filter approach, and the model was proposed for terminal voltages at different SoC. But the models were not expanded to estimate other parameters like the SoC or battery capacity.

A basic ECM of VRFB is proposed in [17,18] with a voltage source that represents the stack voltage, a controlled current source, and a fixed loss resistance representing parasitic losses, reaction resistance, and electrode capacitors. However, it lacks validation of the proposed models. Additionally, in [17,18], the SoC is modeled based on the Coulomb counting method. The Coulomb counting method's accuracy relies on the correct estimation of battery available capacity in each charge and discharge cycle. However, in the long-term use of VRFBs, the available capacity decreases due to ion diffusions across the membrane and the depletion of active materials, a phenomenon known as capacity fading. Therefore, it's more accurate to model VRFB SoC irrespective of its available capacity.

An ECM was proposed in [19] for VRFB with a voltage source representing the stack voltage and a controlled current source. However, the drawback of the proposed ECM is that the parameter identification process is based on estimated values of the battery, and validation of the model is not provided. Additionally, the proposed model did not take account of chemical variation effects on the estimations (the dynamics of the concentration of vanadium ions). A battery model is proposed in [20] as a voltage source in series with internal resistance, but the circuit elements identification method didn't explain clearly.

Some other ECMs are introduced for different types of batteries like Li-ion, for e.g., composite equivalent circuit models [21]. In [21] the battery is modeled by composite equivalent modeling, and its parameters are identified effectively by investigating the hybrid power pulse test. In the composite equivalent model, parallel reverse diodes are employed in the equivalent model to characterize the resistance difference in charging and discharging conditions.

A common procedure for parameter extraction for the VRFB circuit models is electrode overpotentials by electrochemical impedance spectroscopy (EIS), as stated in [22]. The capacitance and resistance in RC models are estimated by measurements under a wide range of frequencies. However, EIS is only applicable to a single cell measurement, and for the large battery stacks, some complement procedures need to apply. Therefore, in this paper, an optimization-based method is employed to identify the ECM's elements, which accurately estimates the circuit elements, as shown in this study's results section.

Adaptive Filtering methods apply filtering algorithms and modern control theory to reduce the noise of estimated parameters [23–29]. Kalman Filters (KFs) are proven common algorithms that are used in the estimation of systems parameters. In [23,24], an improved EKF for SoC estimation of VRFBs is proposed, and the state-space model is based on the ECM of the battery. But, the electrochemical dynamics of the battery like concentrations of Vanadium ions are ignored. In [25–27], the Unscented Kalman Filter (UKF) is used for the estimation of the Li-ion battery parameters. Besides commonly used KFs (EKF and UKF), other estimation methods like Particle Filters (PF) [28,29] are commonly used for modeling highly nonlinear systems.

It is common to modify the KF algorithms for improving the accuracy of estimation of internal battery parameters. For example, in [21] an improved iterate calculation method is proposed to improve the charged state prediction accuracy of the lithium-ion battery packs by introducing a novel splice Kalman filtering algorithm with robust adaptive performance.

In most of the previously published papers [16–20,23–27], only a Constant Current (CC) charging procedure was used to test the ECM of different types of batteries. It will be shown in the current study that although the proposed ECM for the VRFB, models the terminal voltage precisely in CC charging, the proposed ECM can not estimate the terminal voltage accurately in CV charging mode. Therefore, Hybrid Extended Kalman Filter (HEKF) and Particle Filter (PF) algorithms are employed with some modifications to make the proposed ECM applicable for CV charging mode too.

Moreover, an accurate SoC estimation is essential for a battery to ensure its safe operation and prevent it from over-charging or over-discharging [30]. For verifying the consistency of the estimated SoC with HEKF and PF algorithms, the proposed methods will be compared with the electrochemical model and the Coulomb counting estimation method as references.

The paper is organized as follows: Section 2 describes the electrochemical model of the VRFB system and the proposed ECM for VRFB. This section also includes the expressions used in this study for the SoC estimation and battery capacity estimation of the VRFB. This section follows by describing the flow chart of the proposed VRFB parameter estimation procedure and the introduction of HEKF and PF estimation algorithms, which are used for battery parameter estimation in this study. In Section 3, the data of a nine-cell VRFB, i.e., the electrolyte temperature, the electrolyte flow rate, and charging current, are applied as inputs of the battery model, and the proposed ECM is tested by a sample CCCV charging. Further, the HEKF and PF-based estimation methods are used to solve the discrepancy of the ECM with the experimental data of the nine-cell VRFB in CV charging mode. Finally, the SoC and available capacity of the VRFB stack are compared to the Coulomb counting and electrochemical model-based methods. Section 4 concludes the paper.

2. The proposed estimation approach for VRFB parameters

In Section 2.1, the Ordinary Differential Equations (ODEs) of the electrochemical model of the VRFBs are introduced. In Section 2.2 of this section, the ECM for VRFB is proposed, and further, the optimization-based circuit elements parameter identification is introduced.

In Section 2.3, the HEKF and PF algorithms for VRFB parameter estimation are introduced. Finally, in Section 2.4, the expression for estimation of the SoC and available capacity of the battery used in this study are expressed.

2.1. The electrochemical model of VRFB

The electrochemical model of the VRFB is proposed in this subsection. The chemical reactions in VRFB are expressed in equation (1) [31]:

$$VO^{2+} + H_2O \rightarrow VO_2^{+} + 2H^{+} + e^{-} \quad E^0 = +1.0\ V \tag{1a}$$

$$V^{3+} + e^{-} \rightarrow V^{2+} \quad E^0 = -0.26\ V \tag{1b}$$

In which V stands for Vanadium, e is the electron released from the reaction, and E^0 is the standard potential of each positive and negative reactions. The total reaction creates 1.26 Volts which is known as standard Open-Circuit Voltage (OCV) [31]. The Partial Differential Equations (PDE) of VRFB can be reduced to ODEs by discretizing the VRFB cell. The ODEs of the electrochemical model of VRFB are expressed as follows [31]:

$$\frac{dc_2^{cell}}{dt} = \frac{1}{L_{pe}W_{pe}H_{pe}}\left[\frac{Q}{M}\left(c_2^{tank}-c_2^{cell}\right)+\frac{I}{nF}\right] - \frac{1}{W_{pe}}\left[\frac{K_2}{D}c_2^{cell}+\frac{2K_5}{D}c_5^{cell}+\frac{K_4}{D}c_4^{cell}\right] \tag{2a}$$

$$\frac{dc_3^{cell}}{dt} = \frac{1}{L_{pe}W_{pe}H_{pe}}\left[\frac{Q}{M}\left(c_3^{tank}-c_3^{cell}\right)-\frac{I}{nF}\right] - \frac{1}{W_{pe}}\left[\frac{K_3}{D}c_3^{cell}-\frac{3K_5}{D}c_5^{cell}-\frac{2K_4}{D}c_4^{cell}\right] \tag{2b}$$

$$\frac{dc_4^{cell}}{dt} = \frac{1}{L_{pe}W_{pe}H_{pe}}\left[\frac{Q}{M}\left(c_4^{tank}-c_4^{cell}\right)-\frac{I}{nF}\right] - \frac{1}{W_{pe}}\left[\frac{K_4}{D}c_4^{cell}-\frac{3K_2}{D}c_2^{cell}-\frac{2K_3}{D}c_3^{cell}\right] \tag{2c}$$

$$\frac{dc_5^{cell}}{dt} = \frac{1}{L_{pe}W_{pe}H_{pe}}\left[\frac{Q}{M}\left(c_5^{tank}-c_5^{cell}\right)+\frac{I}{nF}\right] - \frac{1}{W_{pe}}\left[\frac{K_5}{D}c_5^{cell}+\frac{2K_2}{D}c_2^{cell}+\frac{K_3}{D}c_3^{cell}\right] \tag{2d}$$

The concentrations of Vanadium ions in tanks derive from:

$$U_{tank}^{-}\frac{dc_2^{tank}}{dt} = Q\left(c_2^{cell}-c_2^{tank}\right) \tag{3a}$$

$$U_{tank}^{-}\frac{dc_3^{tank}}{dt} = Q\left(c_3^{cell}-c_3^{tank}\right) \tag{3b}$$

$$U_{tank}^{+}\frac{dc_4^{tank}}{dt} = Q\left(c_4^{cell}-c_4^{tank}\right) \tag{3c}$$

$$U_{tank}^{+}\frac{dc_5^{tank}}{dt} = Q\left(c_5^{cell}-c_5^{tank}\right) \tag{3d}$$

In equations (2,3) W_{pe}, L_{pe} and H_{pe} are the length, the width and the height of the porous electrode. $\frac{K_2}{D}, \frac{K_3}{D}, \frac{K_4}{D}$, and $\frac{K_5}{D}$ are diffusion coefficients of V^{2+}, V^{3+}, VO^{2+}, and VO_2^{+} ions across the membrane, respectively. F is Faraday constant, M is the number of cells in the battery stack, Q is the electrolyte flow rate, $U_{tank}^{-}, U_{tank}^{+}$ are negative and positive tank's volume and c_2, c_3, c_4, and c_5 are the Vanadium (II),(III),(IV), and (V) concentrations, which are shown for cells and tanks with the corresponding superscripts, constituting all the eight states of the state-space model of the VRFB.

The SoC of the VRFB is estimable using Eqs. (4)–(6) considering SOC of both half-cells calculated based on the concentrations of Vanadium ions present in each electrolyte reservoir during the charge and discharge processes:

$$SoC^{-} = \frac{c_2^{tank}}{c_2^{tank}+c_3^{tank}} \tag{4}$$

$$SoC^{+} = \frac{c_5^{tank}}{c_4^{tank}+c_5^{tank}} \tag{5}$$

Where the Vanadium ion concentrations values are the solution of the VRFB's ODEs (equations 2 and 3). The overall SoC of the VRFB system is the average of $SOC^{-}$and SOC^{+} as expressed in Eq. (6):

$$SoC = \frac{SOC^{-}+SOC^{+}}{2} \tag{6}$$

Eq. (6) is called the electrochemical method for SoC estimation.

2.2. The proposed ECM for VRFBs and the method for identification of ECM's elements

Fig. 1 shows a first-order Resistive-Capacitive (RC) ECM for VRFB. Although higher order of ECMs with more RC parallel elements can add to the accuracy of the ECM, it comes with more complexity and more computation-time for the model. Thus, the first-order ECM is used in this study.

In Fig. 1, the R_s is the series resistant, R_1 is the parallel resistance, and C_1 is the parallel capacitance of the first-order ECM.

For a parallel RC impedance, the KCL can be written as:

$$C_i\frac{dV_1}{dt}+\frac{V_1}{R_i} = I \tag{7}$$

In which V_1 is the voltage across each of RC parallel impedances, and I is the battery current.

The discrete form of the voltage of each parallel RC impedance can be written as [24]:

$$V_i(k) = \exp\left(-\frac{\Delta t}{R_iC_i}\right)V_i(k-1)\left[1-\exp\left(-\frac{\Delta t}{R_iC_i}\right)\right]R_iI(k-1) \tag{8}$$

Where k is discrete-time instances, and Δt is time intervals.

In the first-order RC model, the battery terminal voltage is as follows in charging mode:

$$V_T = M.V_{oc}+V_1+R_sI \tag{9}$$

Where M is the number of cells, and V_1 is the voltage across the parallel RC impedance, which is determined by Eq. (8). In this research study, the equations are formulated in charging mode; however, the proposed method is applicable for discharging mode too. In discharging mode, the signs of V_1 and I are negative.

Fig. (2) shows the flowchart of the proposed procedure to estimate the parameters of VRFBs in this study.

In Eq. (9), the open-circuit voltage, V_{oc} can be estimated and be replaced from the results of the electrochemical model as expressed in Eq. (10):

$$V_{oc} = M\left[E_0+\frac{2RT}{nF}Ln\left(\frac{c_2^{cell}(C_{H^+})^2}{c_3^{cell}}\right)\right] \tag{10}$$

Where c_2^{cell} and $c_3^{cell}$are Vanadium II and III concentrations of cells, and c_{H^+} is concentration of Hydrogen in the electrolyte solution. E_0 is standard cell potential equal to 1.4 Volts for SoC of 50% [28], n is the number of electrons transferred in the cell reaction, R is gas constant, T is the electrolyte temperature in Kelvin. In the current study, an optimization-based method is used for determining the values of circuit elements of the first-order ECM (R_s, R_1, and C_1), as follows.

The Thevenin impedance of the first-order ECM is as follows:

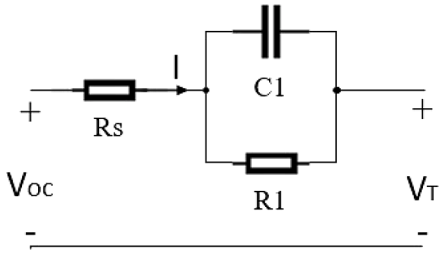

Fig. 1. first-order RC ECM for VRFBs.

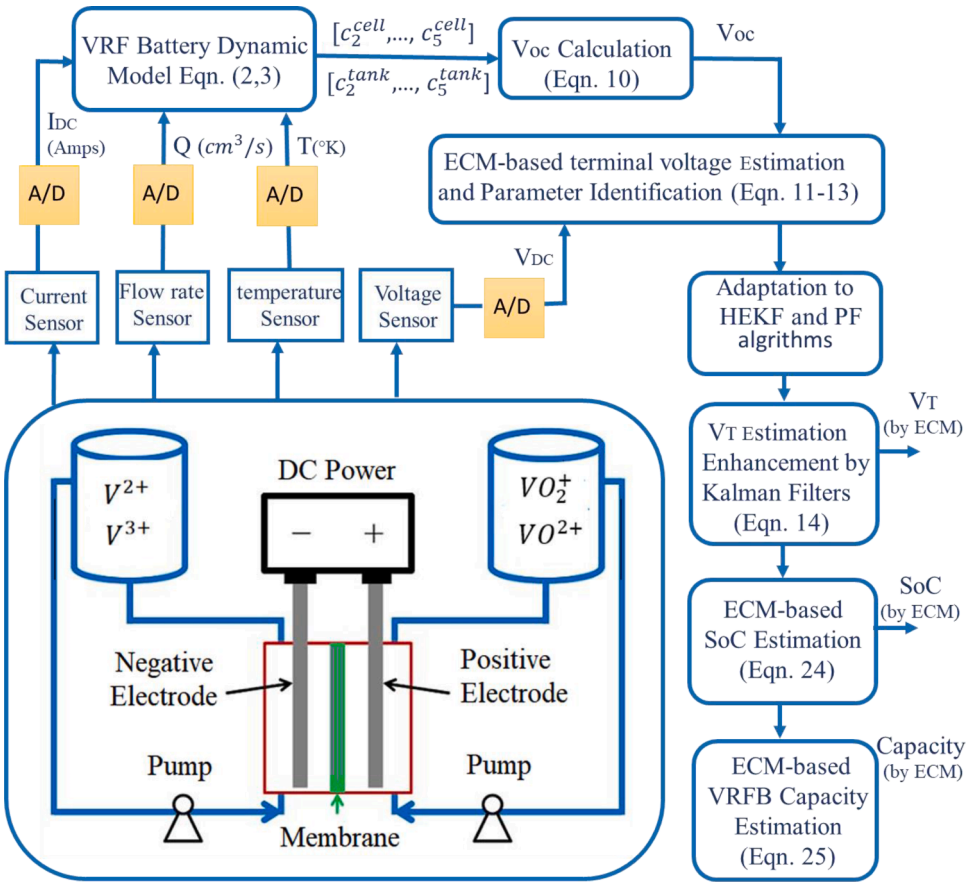

Fig. 2. The proposed unified VRFB Electrochemical ECM-based model flowchart.

$$Z(j\omega) = R_s + \frac{R_1\left(\frac{1}{j\omega C_1}\right)}{R_1 + \left(\frac{1}{j\omega C_1}\right)} \tag{11}$$

On the other hand, the Thevenin equivalent impedances considering KVL is expressed in Eq. (12):

$$Z_{th}(j\omega) = Avg((V_T - MV_{oc})/I) \tag{12}$$

Where *Avg* is the average of the Thevenin impedances on all sample data. The circuit elements R_s, R_1, and C_1 can be estimated by minimizing the error between the two impedances i.e., Eqs. (11) and (12) as shown in equation (13):

$$Minimize\ Z_{th}(j\omega) - Z(j\omega) \tag{13a}$$

$$Subjected\ to\ R_s, R_1,\ and\ C_1 > 0 \tag{13b}$$

The constraints of the above optimization express that the series and parallel RC circuit elements are positive. In Eq. (12), $Z_{th}(j\omega)$ is assumed as the average (*Avg*) of the Thevenin impedance for each sample. For each discrete sample time (k), there are corresponding circuit elements $[R_s(k), R_1(k),$ and $C_1(k)]$. However, unique values for circuit elements are needed to preset before using the battery model for simulations. Therefore, the average value of the samples is considered in the current study. Eq. (12) shows that the Thevenin impedance is a function of the charging current (I).

Based on experimental results, it will be shown that although the proposed optimization-based model is accurate in CC charging, it is not so in CV charging mode where the charging current varies. Hence, two adaptive Kalman filters (HEKF, and PF) are applied to the ECM to solve the propseod model's discrepancies with the experimental data of the VRFB in CV charging mode.

2.3. The proposed adaptive Kalman Filter algorithms for the ECM of VRFBs

To solve the inconsistency of the proposed ECM in CV charging mode, two nonlinear Kalman Filters (KFs) are employed in this study to estimate the parameters of VRFBs. The other benefit of using the KFs is decreasing the estimation noise of the battery parameters. The VRFB parameters are estimated, considering the ECM state-space system using equation (14). The state-space model of the first-order ECM in charging mode can be expressed as equation (14):

$$\frac{dV_1}{dt} = -\frac{V_1}{R_1C_1} + \frac{I}{C_1} \tag{14a}$$

$$V_T = MV_{oc} + V_1 + R_sI \tag{14b}$$

Where V_1 is the state variable, I is the battery current (input of the system), and V_T is the battery terminal voltage (output of the system). Note that the open-circuit voltage (V_{oc}) in equation 14 should be replaced from Eq. (10), which is resulted from the VRFB electrochemical model, i.e., equation 2,3).

2.3.1. Hybrid Extended Kalman Filter (HEKF)

Most of the real engineering systems can be identified by continuous-time dynamics, however, the output measurements are sometimes in discrete form. For these kinds of systems, the hybrid form of EKF, namely HEKF, is suitable [29]. By using HEKF, there is no need to discretize the continuous-time system to adapt to the conventional EKF, which results in simpler mathematical modeling and less computation-time.

EKF algorithm is common for nonlinear systems in literature because of the ease of modeling compared to other methods like the PF

algorithm. However, the other reason why HEKF is used in this paper is that the system definition is simply modifiable in the HEKF algorithm. Thus, the HEKF is chosen in this study because there are essential changes to the proposed ECM to be applicable for the CV charging mode too.

On the other hand, the PF algorithm is another suitable estimation algorithm that is commonly used for highly nonlinear systems. However, the PF algorithm is independent of the system model; therefore, the system definition is not modifiable in contrast to the EKF and HEFK algorithms. Both the HEKF and PF estimation algorithms are used in this study to estimate the VRFB parameters, and the two estimation methods' efficiency in the estimation of the terminal voltage and the SoC of the VRFBs are compared.

The system equations with continuous-time dynamics and discrete-time measurements are described in equation (15):

$$\dot{x} = f(x, u, w, t) \tag{15a}$$

$$y_k = h_k(x_k, v_k) \tag{15b}$$

$$w(t) \sim (0, Q) \tag{15c}$$

$$v_k \sim (0, R_k) \tag{15d}$$

Where x: $[V_1]$ is the state variable vector, u: [I] is input, $y_k : [V_T]$ is considered as output. w,v_k are process and white noise from measurement has covariance of Q and R_k respectively. The HEKF algorithm is described in the following section:

2.3.1.1. Initialize the filter as Eq. (16). .

$$\begin{aligned} \widehat{x}_0^+ &= E[x_0] \\ P_0^+ &= E\left[\left(x_0 - \widehat{x}_0^+\right)\left(x_0 - \widehat{x}_0^+\right)^T\right] \end{aligned} \tag{16}$$

2.3.1.2. For k=1, 2, … perform the following. .

2.3.1.2.1. Integrate the state estimate and its covariance from time $(k-1)^+$ to time k^- as described in equation (17). .

$$\dot{\widehat{x}} = f(\widehat{x}, u, 0, t) \tag{17a}$$

$$\dot{P} = AP + P^T + LQL^T \tag{17b}$$

Where P is the estimation covariance matrix, T denotes the transpose of matrices, Q is the process covariance, and L is Jacobian Matrix. This integration begins with $\widehat{x} = \widehat{x}_{k-1}^+$ and $P = P_{k-1}^+$. At the end of this integration $\widehat{x} = \widehat{x}_k^-$ and $P = P_k^-$. R is not included in the equation for $\dot{P}$ because during the integration of P between actual measurement times, its value is not updated.

2.3.1.2.2. At the k^{th} sampling instance, the gain, the posteriori, and estimation covariance are as equation (18). .

$$K_k = P_k^- H_k^T \left(H_k P_k^- H_k^T + M_k R_d M_k^T\right)^{-1} \tag{18a}$$

$$x_k^+ = \widehat{x}_k^- + K_k\left(\mathrm{y}_k - h_k\left(\widehat{x}_k^-, 0, t_k\right)\right) \tag{18b}$$

$$P_k^+ = (I - K_k H_k) P_k^- (I - K_k H_k)^T + K_k M_k R_k M_k^T K_k^T \tag{18c}$$

H_k and M_k are the partial derivatives of $h_k(x_k, v_k)$ with respect to x_k and v_k and are both evaluated at $\widehat{x}_k^-$.

2.3.2. Particle filter (PF)

The PF algorithm is also recognized by some other names like bootstrap filtering [32]. The PF algorithm is as follows:

2.3.2.1. First, if the system is continuous, it should be discretized. .

$$x_{k+1} = f_k(x_k, \omega_k) \tag{19a}$$

$$y_k = h_k(x_k, v_k) \tag{19b}$$

Where ω_k and v_k are independent white noise processes with known pdf, which is a probability distribution (the likelihood of an outcome) for a discrete random variable.

2.3.2.2. Generate random N particle ($x_{0,i}^+$). .

2.3.2.3. For k=1, 2, the following method is followed. .

2.3.2.3.1. Propagation to obtain a priori particles ($x_{k,i}^-$). .

$$x_{k,i}^- = f_{k-1}\left(x_{k-1,i}^+, \omega_{k-1,i}\right) \quad (i = 1, \ldots, N) \tag{20}$$

2.3.2.3.2. Calculate the likelihood q_i for each particle by evaluating the pdf $p(y_k | x_{k,i}^-)$ on the nonlinear measurement equation. .

2.3.2.3.3. Scale the relative likelihood in the previous part. .

$$q_i = \frac{q_i}{\sum_{j=1}^{N} q_j} \tag{21}$$

Where the sum of all the likelihoods is equal to 1.

2.3.2.3.4. Resampling step: Generate a set of a posteriori particles ($x_{k,i}^+$) based on the relative likelihood q_i. .

2.3.2.3.5. Having all sets of particles ($x_{k,i}^+$) according to the pdf $p(x_k | y_k)$, one can calculate any statistical measure of this pdf, for example, the mean and the covariance. .

2.4. The estimation of SoC and available capacity of VRFBs

The proposed ECM method in Section 2.2 can be used to estimate the SoC and available capacity of VRFBs. The conventional mapping method to find the SoC based on the Open-Circuit Voltage (OCV) is not an accurate method because it accompanies with some errors due to interrupting the battery's charging or discharging to measure OCV. It also mentioned that while the charge accumulates in the electrolyte of reservoir tanks, It is more accurate to estimate the SoC of VRFBs considering the Vanadium ions concentrations.

Further, the proposed ECM method using the HEKF and PF algorithms (ECM-HEKF and ECM-PF methods) is employed to estimate SoC and battery available capacity. Eq. (9) can be used to estimate the OCV of a cell based on the proposed ECM as follows in charging mode:

$$\widehat{V_{oc}} = \left(\widehat{V_T} - \widehat{V_1} - \widehat{R}_s I\right) \Big/ M \tag{22}$$

Where $\widehat{V_1}$ is the estimated voltage of RC parallel impedance, and $\widehat{V_T}$ is estimated value of terminal voltage, and $\widehat{R}_s$ is the optimal series resistance resulted from the optimization equation 13. The charging current (I) is constant in CC charging mode while it varies in CV charging, which will be defined further by Eq. (27) for CV charging mode. In discharging mode, however, the estimated OCV ($\widehat{V_{oc}}$) of a cell is:

$$\widehat{V_{oc}} = \left(V_T + \widehat{V_1} + \widehat{R}_s I\right) / \mathrm{M} \tag{23}$$

Knowing the estimated value of open-circuit voltage $\widehat{V_{oc}}$ by Eqs. (22) and (23), the SoC of the VRFB can be estimated by the modified Nernst equation, assuming that all the vanadium species are fully balanced in the VRFB system as Eq. (24):

$$\widehat{SoC} = \frac{\exp\left[\frac{nF}{2RT}\left(\widehat{V_{oc}} - 1.4\right)\right]}{1 + \exp\left[\frac{nF}{2RT}\left(\widehat{V_{oc}} - 1.4\right)\right]} \tag{24}$$

The available capacity of the VRFB can be derived from the results of SoC estimation, as expressed in Eq. (25):

$$\text{Available Capacity} = \frac{\int I(t)dt}{\left[\widehat{SoC}(K) - \widehat{SoC}(K-1)\right]} \tag{25}$$

In Eq. 25, the SoC estimated value ($\widehat{SoC}$) is derived from the proposed ECM and not the Coulomb counting method. Then the SoC will be estimated by the proposed ECM-HEKF or ECM-PF method, the resulting estimated value ($\widehat{SoC}$) can be used to estimate the available capacity of VRFBs according to Eq. 25.

3. Verification of the proposed estimation method for VRFB's parameter using the experimental data of a VRFB stack

In this section, the ECM reliability is verified by a nine-cell VRFB. The VRFB prototype system setup is shown in Fig (3). The setup consists of positive and negative side reservoir tanks with an equal amount of electrolyte, which is a solution of Vanadium and sulfuric acid. Two pumps are used for electrolyte circulation to the battery stack and back to reservoir tanks. Two temperature sensors, two flow rate sensors, two pressure sensors, a DC current sensor, and a voltage sensor are used for monitoring of the VRFB system. For electrolyte flow rate control, a Battery Management System (BMS) controls the speed of the pumps, and hence the flow rate of electrolytes using two Variable Frequency Drives (VFDs) controlled digitally.

In Section 3.1, the results of the ODEs (equations 2 and 3) describing VRFB's electrochemical behavior for the nine-cell VRFB stack are provided. In Section 3.2 of this section, the proposed ECM for VRFB is verified compared to the experimentally measured data of the nine-cell VRFB stack. The estimation algorithms, HEKF and PF, which are introduced in Section 2, are used to solve the experimental data's discrepancies with the proposed ECM in CV charging mode. In Section 3.3, the HEKF based and PF-based ECM methods are used to estimate SoC and battery capacity, and the results are compared to the Coulomb counting and electrochemical model-based method.

3.1. The results of ODEs of VRFB electrochemical model

In Table 1, the parameters used in the proposed VRFB electrochemical model are shown. Table 2 shows the error of the sensors (from the datasheets), which are used in the battery experiments.

A sample CCCV charging data is used for verification of the proposed estimation methods, as shown in Fig. 4. According to Fig. 4, the first stage is constant current charging, but the current profile is not completely smooth, and it has some fluctuation which is because of the DC current sensor error. In the first stage of CCCV charging, the battery

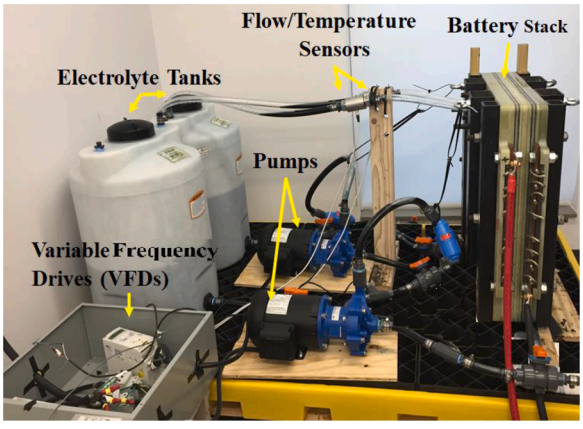

Fig 3. The nine-cell VRFB setup used for data acquisition and verification of results.

Table 1
The parameters in the proposed VRFB model.

Symbol	Quantity	Value
P	Rated power	2.25 (kW)
i_n	Nominal current density	58 (mA cm^{-2})
M	No. of cells in the stack	9
U_{tank}	Volume of tank electrolyte	25 (gallons)
L_{pe}	Length of porous electrode	0.4 (m)
W_{pe}	Width of porous electrode	0.25 (m)
H_{pe}	Height of porous electrode	0.003 (m)
r^{cell}	Cell internal resistivity	2 (Ωcm^2)
F	Faraday constant	96485 ($Cmol^{-1}$)
R	Gas constant	8.314 ($J\ mol^{-1}K^{-1}$)
$(\frac{K_2}{D})$	Diffusion coefficient of V(II)	3.17e-6 (cms^{-1})
$(\frac{K_3}{D})$	Diffusion coefficient of V(III)	0.72e-6 (cms^{-1})
$(\frac{K_4}{D})$	Diffusion coefficient of V(IV)	2e-6 (cms^{-1})
$(\frac{K_5}{D})$	Diffusion coefficient of V(V)	1.25e-6 (cms^{-1})
ρ_{el}	Electrolyte density	1354 ($kg.m^{-3}$)
η	Electrolyte viscosity	4.928e-3 (Pa.s)
d_{fb}	Electrode fiber diameter	17.6e-4 (cm)
ϵ	Electrode porosity	0.93

Table 2
Error of Sensors used in VRFB experiments.

Sensor	error
Electrolyte Flow rate	±2% of measured value
Electrolyte Temperature	2.5 (^oK)
DC Voltage	±1% of measured value
DC Current	±2% of measured value

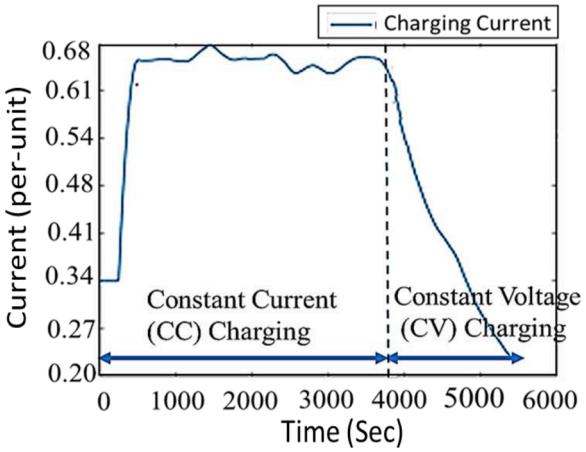

Fig. 4. The sample CCCV charging current profile used for verification of the proposed estimation method.

charges with constant current (bulk charging) until the voltage level reaches the preset value of voltage (1.7 Volts per cell in this study). The charging process will continue with Constant Voltage (CV) in the second stage.

The VRFB stack under test has porous graphite felts as positive and negative electrodes, and the membrane is a commercial membrane "VANADion". The dimension of porous electrodes is 40 × 25 × .3 (cm) each.

The resulted Vanadium II, III ions concentrations (mol/liter), which are the solution of ODEs in equations (2,3) are shown in Fig. 5 (a,b).

The graphs of all the VRFB system states are not shown because the

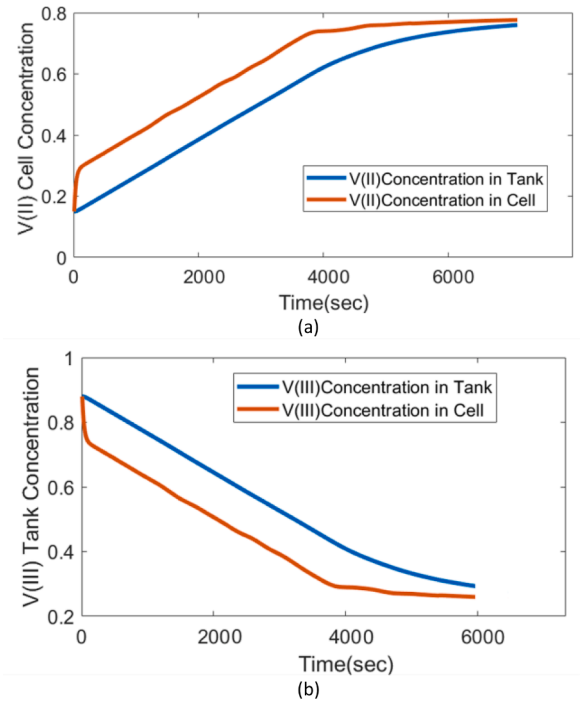

Fig. 5. (a) Vanadium II concentrations, (b) Vanadium III concentrations, resulted from ODEs (Eqs. 2 and 3).

graphs of the other six states of the VRFB state-space system are almost the same as these two states, which are shown in Fig. 5 (a, b).

3.2. *Verification of the proposed ECM using the nine-cell VRFB's terminal voltage*

The ECM for VRFB is proposed in Section 2. It is compared with the measured experimental data of the nine-cell VRFB unit in this subsection for verifying the proposed model. The result of the comparison is shown in Fig. 6. The optimal values of the ECM elements have resulted from equation 13, and are shown in Table 3 as follows

Fig. 6 shows the comparison of the ECM-based terminal voltage model with the nine-cell VRFB unit's experimental data. As shown in Fig. 6, the battery terminal voltage resulted from the ECM is accurate enough in CC charging (left side of Fig. 6), but it is not accurate in CV

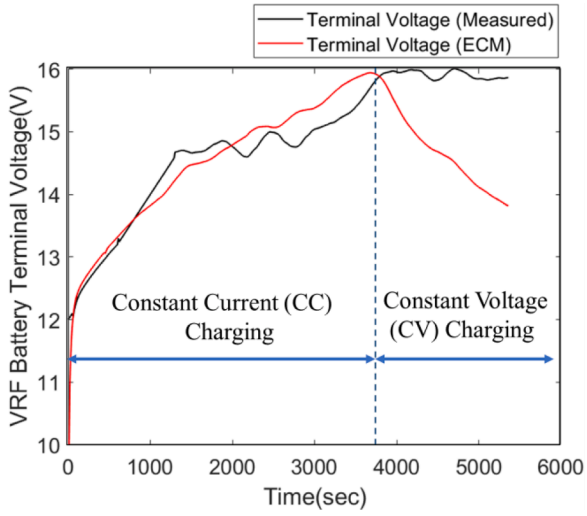

Fig. 6. verification of ECM-based VRFB terminal voltage of the nine-cell VRFB stack.

Table 3
Optimal ECM elements for the nine-cell VRFB unit.

Series Resistance	Parallel Resistance	Parallel Capacitance
0.0406 Ω	30.86 Ω	1.09e+5 F

charging (right side of Fig. 6). This inaccuracy is because the method used for parameter identification based on the average of Thevenin equivalence impedances (proposed in Section 2) does not hold well in CV charging mode.

As mentioned, the charging current is variable in CV mode, so the ECM loses accuracy in this mode. Therefore, to address the mentioned inaccuracy problem, a recursive function is proposed for the HEKF algorithm in CV mode to model charging current reduction in this mode, which reduces the discrepancies of the model with the experimental data in CV mode.

In CV mode, the terminal voltage is constant:

$$V_T(k) = V_T(k-1) \tag{26}$$

In the CV charging mode, the charging current reduces recursively to keep the terminal voltage constant. Using equation 14, the charging current can be updated recursively as:

$$I(k) = I(k-1) \tag{27}$$

$$- \left[MV_{oc}(k) - MV_{oc}(k-1) + V_1(k) - V_1(k-1)\right]/R_s$$

Where $V_{oc}(k)$ is assumed a single cell open-circuit voltage. This change to the ECM in CV mode is applied by modifying HEKF's algorithms. For the HEKF-based estimations, it is possible to apply necessary changes to the system model by modifying the HEKF algorithm. However, this is not possible for the ECM-PF-based model because the PF algorithm is independent of the system model, and it is not possible to apply any change to the system by modifying the PF algorithm. Therefore, another solution is considered for PF based estimation in this study considering the fact that the voltage is constant in CV charging mode (as Eq. (26)).

Fig. 7 shows the resulting terminal voltage model by ECM, ECM-HEKF, and ECM-PF algorithms compared to the measured experimental data of the nine-cell VRFB unit.

According to Fig. 7, Although the ECM-based terminal voltage models closely match the experimental data in CC charging (left side of Fig. 7), the ECM-based estimation is not accurate in CV charging (right side of Fig. 7). On the other hand, assigning the recursive function to the ECM-HEKF and applying the mentioned condition to the ECM-PF algorithm consistently improved the proposed ECM inaccuracy in the CV

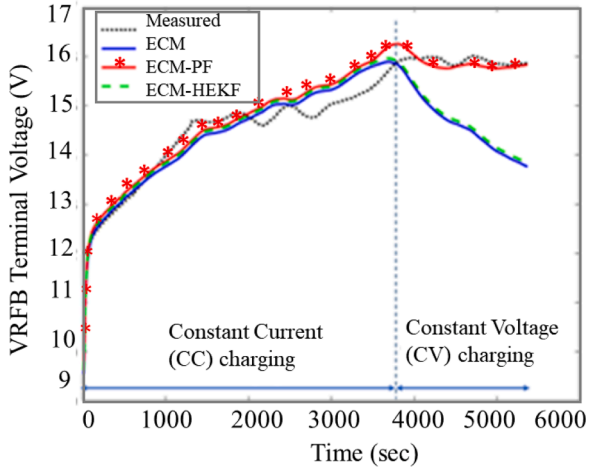

Fig. 7. Comparison of estimated terminal voltage by different methods with experimental data of the nine-cell VRFB stack.

mode.

As a result, the proposed ECM-HEKF- and ECM-PF-based terminal voltage model closely matches the nine-cell VRFB unit's experimental data in both CC and CV charging modes. The remaining deviation in the estimated values is mainly because of sensor measurement errors used in VRFB's experiments and inherent error in VRFB ODE-base electrochemical model, which cannot completely fit the experimentally measured data. As mentioned, the difference between the HEKF and PF algorithms is that in the HEKF algorithm, it is possible to make changes to the algorithm directly to adapt it for any kind of battery charging like the CV mode. However, the PF algorithm is independent of the system model, and it is not possible to adapt it directly. This can be concluded as an advantage for the HEKF algorithm regarding its modifiable algorithm. The average deviation of each method in estimating the terminal voltage of the nine-cell VRBF is shown in Table 4.

Table 4 shows that both of the HEKF and PF-based methods significantly improve the accuracy of the estimated terminal voltage of the nine-cell VRFB in a sample CCCV charging.

3.3. The use of proposed KF methods in estimation of the SoC and available capacity of VRFBs

According to improvements by HEKF and PF methods to the initially proposed ECM, and the reliability of the estimation for the VRFB's terminal voltage, these KF methods are extended to estimate other parameters of VRFBs like the SoC and the available capacity of the nine-cell VRFB unit.

The estimated SoC by these KF methods are compared with the Coulomb counting and the electrochemical ODE-base method as the reference in Fig. 8. The electrochemical-based SoC estimation algorithm is more time-consuming and it has more burden of mathematical modeling than the ECM approaches. However, the electrochemical model is used as reference and compared with the other estimation methods in this study, because it is proven as one of the most accurate methods for SoC estimation of the redox flow batteries.

As Fig. 8 shows, the result of estimated SoC with initially proposed ECM is not accurate in CV charging mode. However, according to Fig. 8, the SoC of VRFB estimated by the proposed ECM-HEKF and ECM-PF methods are accurate in both CC and CV charging modes with low deviations. The remaining deviation is acceptable, considering inevitable errors of sensors and the fact that the dynamic electrochemical model does not fit completely to the experimental data.

Commonly computational complexities involved with PF-based estimations are known to be one of the major constraints to their widespread use. On the other hand, EKF-based estimations are easier to define, but sometimes PF has better estimations for highly nonlinear systems. Table 5 shows the average deviations of each method to estimate the SoC of the VRFB under test.

According to Table (4,5), the estimations of terminal voltage and SoC of VRFBs by the ECM-HEKF and ECM-PF algorithms are more accurate than other methods since these algorithms are modified (improved) in CV mode leading to enhancement of estimations. The remaining deviation of HEKF and PF based methods are mainly because of sensor measurement errors used in VRFB's experimental setup and the inherent error in VRFB's ODE-based electrochemical model to fit the experimental data, and that the average of optimal equivalent circuit elements is used in this study.

Therefore, the ECM-HEKF and ECM-PF algorithms are expanded to estimate the available capacity of the nine-cell VRFB by Eq. (25). The resulting available capacity of nine-cells VRFB is estimated as about 2.05 kWh, assuming tanks containing 25 gallons of electrolyte each. However, VRFB's available energy depends on the volume of the electrolyte in the reservoir tanks, which considers as RBF's benefit in which power and energy sizing are decoupled. As mentioned, in the long-term use of VRFBs, the available capacity reduces due to ion diffusions across the membrane and the depletion of active materials (capacity fading).

The proposed HEKF and PF-based ECM algorithms are accurate models that can be used for any VRFB with any number of cells and stack configuration. The proposed algorithm was formulated for charging mode, but the method can be used in discharging mode as well by minor changes in signs of quantities in the proposed equations.

Table 4
The average deviation of each method in estimation of the nine-cell VRFB terminal voltage.

Average deviation of ECM-HEKF	The average deviation of ECM-PF	The average deviation of initial ECM
0.88%	0.79%	7.21%

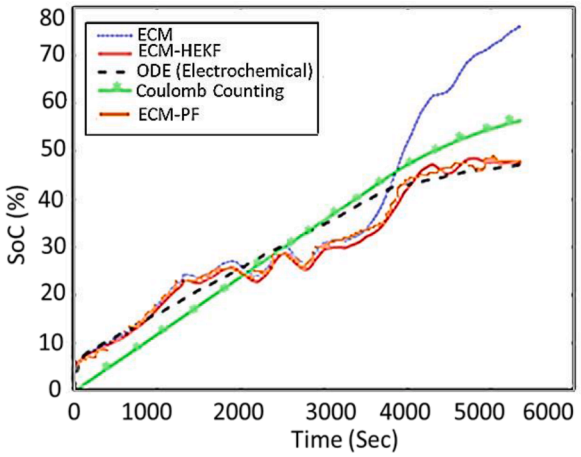

Fig. 8. Comparison of estimated SoC with the proposed methods with the electrochemical method and the Coulomb counting methods.

Table 5
The average deviation of each method in the estimation of SoC of the nine-cell VRFB unit.

The average deviation of ECM-HEKF	The average deviation of ECM-PF	The average deviation of ECM	The average deviation of Coulomb counting
4.4%	4.2%	23.7%	7.4%

4. Conclusion

A new circuit equivalent model unified with electrochemical model is introduced for VRFBs in this study for parameter estimation of the battery. The accuracy of the proposed ECM and circuit elements identification method is verified on both CC and CV charging modes using a sample CCCV charging data. As the ECM uses the average of circuit elements in all samples during charge/discharging, the ECM shows a considerable deviation in CV charging mode. To address this deviation in CV mode, HEKF and PF Kalman filter-based estimation algorithms are employed to enhance the accuracy of CV mode estimations. Moreover, a recursive function is defined for the HEKF algorithm in CV charging mode to keep the terminal voltage constant while modeling the reduction in current during the constant voltage. The results show HEKF and PF estimation methods consistently improve the estimated battery terminal voltage compared to the initially introduced ECM, during the CV charging mode. For the sample CCCV charging, results show the average deviation of 0.88% for the ECM-HEKF method, and the average deviation of 0.79% for the ECM-PF method in estimating the battery terminal voltage, while the initially proposed ECM has a deviation of 7.21% compared to the experimental data. The negligible deviation of HEKF and PF-based methods is mainly because of sensor measurement errors

used in VRFB's experimental setup and the inherent error in VRFB's ODE-based electrochemical model to fit the experimental data.

Further, the proposed procedure is extended to estimate the SoC of the battery. According to the results, the ECM-HEKF and ECM-PF algorithms based SoC estimation for the nine-cell VRFB show more accuracy compared to the estimated SoC by the Coulomb counting method (while the electrochemical model is taken as the reference). The results show the average deviation of 4.2% and 4.4% for the PF and HEKF based methods compare to the SoC estimation by the electrochemical model, while the average deviation of the Coulomb counting method is about 7.4%. Therefore, it can be concluded that the proposed HEKF and PF-based ECM algorithms are more accurate models for VRFB's parameter estimation, i.e., SoC, terminal voltage, and battery capacity.

CRediT authorship contribution statement

Bahman Khaki: Conceptualization, Methodology, Data curation, Formal analysis, Investigation, Software, Validation, Writing - original draft. **Pritam Das:** Conceptualization, Investigation, Validation, Writing - original draft.

Declaration of Competing Interest

The authors declare that they have no known competing financial interests or personal relationships that could have appeared to influence the work reported in this paper.

References

[1] Q. Xu, T.S. Zhao, P.K. Leung, Numerical investigations of flow field designs for vanadium redox flow batteries, Appl. Energy 105 (2013) 47–56.
[2] J. Kim, H. Park, Experimental analysis of discharge characteristics in vanadium redox flow battery, Appl. Energy 206 (2017) 451–457.
[3] T. Wang, J. Fu, M. Zheng, Z. Yu, Dynamic control strategy for the electrolyte flow rate of vanadium redox flow batteries, Appl. Energy (2017).
[4] E. Sum, M. Skyllas-Kazacos, A study of the V(II)/V(III) redox couple for redox flow cell applications, J. Power Sources 15 (1985) 179–190.
[5] E. Sum, M. Rychcik, M. Skyllas-Kazacos, Investigation of the V(V)/V(IV) system for use in the positive half-cell of a redox battery, J. Power Sources 16 (1985) 85–95.
[6] B. Sun, M. Skyllas-Kazakos, Chemical modification and electrochemical behaviour of graphite fibre in acidic vanadium solution, Electrochim. Acta 36 (2007).
[7] F. Rahman, M. Skyllas-Kazacos, Vanadium redox battery: Positive half-cell electrolyte studies, J. Power Sources 189 (2009) 1212–1219.
[8] M. Vijayakumar, L. Li, G. Graff, J. Liu, H. Zhang, Z. Yang, J.Z. Hu, Towards understanding the poor thermal stability of V5+ electrolyte solution in Vanadium Redox Flow Batteries, J. Power Sources (2011) 196.
[9] S. Kim, M. Vijayakumar, W. Wang, J. Zhang, B. Chen, Z. Nie, F. Chen, J. Hu, L. Li, Z. Yang, Chloride supporting electrolytes for all-vanadium redox flow batteries, Phys. Chem. Chem. Phys. 13 (2011) 18186–18193.
[10] KW. Knehr, E.C. Kumbur, Open circuit voltage of vanadium redox flow batteries: discrepancy between models and experiments, Electrochem. Commun. 13 (4) (April 2011) 342–345.
[11] T. Sukkar, M. Skyllas-Kazacos, Water transfer behavior across cation exchange membrane in the vanadium redox battery, J. Membr. Sci. 222 (2003) 235.
[12] H. Al-Fetlawi, A.A. Shah, F.C. Walsh, Non-isothermal modeling of the all-vanadium redox flow battery, Electrochim. Acta 55 (2009) 78–89.
[13] M.-. Li, T. Funaki, T. Hikihara, A study of output terminal voltage modeling for redox flow battery based on charge and discharge experiments, in: 2007 Power Conversion Conference, 2007, pp. 221–225.
[14] A.A. Shah, M.J. Watt-Smith, F.C. Walsh, A dynamic performance model for redox-flow batteries involving soluble species, Electrochim. Acta 53 (2008) 8087–8100.
[15] M.R Mohamed, H Ahmad, M.N.Abu Seman, S Razali, MS Najib, Electrical circuit model of a vanadium redox flow battery using extended Kalman filter, J. Power Sources 239 (2013) 284–293.
[16] Z. Wei, K.J. Tseng, N. Wai, T.M. Lim, M. Skyllas-Kazacos, Adaptive estimation of State of charge and capacity with online identified battery model for vanadium redox flow battery, J. Power Sources 332 (2016) 389–398.
[17] L. Barote, C. Marinescu, A new control method for VRB SOC estimation in standalone wind energy systems, in: 2009 International Conference on Clean Electrical Power, Capri, 2009, pp. 253–257.
[18] L. Barote, C. Marinescu, M. Georgescu, VRB modeling for storage in standalone wind energy systems, in: 2009 IEEE PowerTech, 2009, pp. 1–6.
[19] J. Chahwan, C. Abbey, G. Joos, VRB modelling for the study of output terminal voltages, internal losses and performance, in: 2007 IEEE Canada Electrical Power Conference, Montreal, Que., 2007, pp. 387–392.
[20] R.L. Fares, J.P. Meyers, M.E. Webber, A dynamic model-based estimate of the value of a vanadium redox flow battery for frequency regulation in Texas, Appl. Energy 113 (2014) 189–198.
[21] S. Wang, C. Fernandez, C. Yu, Y. Fan, W. Cao, D.-I. Stroe, A novel charged state prediction method of the lithium ion battery packs based on the composite equivalent modeling and improved splice Kalman filtering algorithm, J. Power Sources 471 (2020), 228450.
[22] J.G. Zhu, Z.C. Sun, XZ. Wei, H.F. Dai, A new lithium-ion battery internal temperature online estimate method based on electrochemical impedance spectroscopy measurement, J. Power Sources (2015) 274.
[23] Ya Qiu, Xin Li, Wei Chen, Ze-min Duan, Ling Yu, State of charge estimation of vanadium redox battery based on improved extended Kalman filter, ISA Trans. 94 (2019) 326–337.
[24] Zhongbao Wei, King Jet Tseng, Nyunt Wai, Tuti Mariana Lim, Maria Skyllas-Kazacos, Adaptive estimation of State of charge and capacity with online identified battery model for vanadium redox flow battery, J. Power Sources 332 (2016) 389–398.
[25] Zewang Chen, Liwen Yang, Xiaobing Zhao, Online State of charge estimation of Li-ion battery based on an improved unscented Kalman filter approach, Appl. Math. Modell. 70 (2019) 532–544.
[26] Hongwen He, Yuanpeng Hongzhou Qin, Karpenko Shui, Oleksandr lithium-ion battery SoC estimation with UKF and RTOS μCOS-II platform, Energy Procedia 612014 (2020) 468–471.
[27] Yong Tian, Bizhong Xia, Wei Sun, Zhihui Xu, Weiwei Zheng, A modified model-based state of charge estimation of power lithium-ion batteries using unscented Kalman filter, J. Power Sources 27015 (December 2014) 619–626.
[28] S. Yin, X. Zhu, Intelligent particle filter and its application to fault detection of nonlinear system, IEEE Trans. Indust. Electron. 62 (6) (June 2015) 3852–3861.
[29] Dan Simon, Optimal State Estimation: Kalman, H Infinity, and Nonlinear Approaches, John Wiley & Sons, Jun 19, 2006.
[30] M.A. Hannan, M.S.H. Lipu, A. Hussain, M.H. Saad, Neural network approach for estimating state of charge of lithium-ion battery using backtracking search algorithm, IEEE Access 6 (2018) 10069–10079.
[31] Yifeng Skyllas-Kazacos Li, Bao Maria, Jie, A dynamic plug flow reactor model for a vanadium redox flow battery cell, J. Power Sources 311 (April 2016) 57–67.
[32] N. Gordon, D. Salmond, A. Smith, Novel approach to nonlinear/non Gaussian Bayesian state estimation, IEEE Proc.-F 140 (2) (1993).

Bahman Khaki was born in Tehran, Iran. He graduated with an M.Sc. degree in Electrical Engineering in Tehran, Iran, and he is studying Ph.D. in Electrical Engineering at the State University of New York at Binghamton, USA. His special fields of interest include power systems and power electronics research with a focus on renewable energy studies, battery energy storage systems, and applying mathematical methods/algorithms and control sub-systems to these systems.

Pritam Das received the M.Sc. and Ph.D. degrees in electrical engineering from the University of Western Ontario, London, ON, Canada, in 2005 and 2010, respectively. From 2010 to 2011, he was a Postdoctoral Fellow with the Queen's Centre for Energy and Power Electronics Research (ePOWER), Queen's University, Kingston, ON, Canada, and with PE consultants, Kingston. From 2013 to 2017, he was an Assistant Professor with the Department of Electrical and Computer Engineering, National University of Singapore, Singapore. He is currently an Assistant Professor with the Department of Electrical and Computer Engineering, State University of New York, Binghamton, NY, USA. His present research interests include wide bandgap device-based single-stage high power resonant converters for behind-the-meter grid-connected energy storage systems, dc Data Centers, ac fast chargers for heavy electric vehicles, reliable modular multi-level converters for off-shore wind power and energy storage systems.